Columbia Environmental Research Center

Aquatic Habitat Mapping with an Acoustic Doppler Current Profiler: Considerations for Data Quality

By David Gaeuman and Robert B. Jacobson

Open-File Report 2005-1163

U.S. Department of the Interior
U.S. Geological Survey

Contents

Figures

Conversion Factors

Multiply	By	To obtain
Length		
centimeter (cm)	0.3937	inch (in.)
meter (m)	3.2808	foot (ft)
kilometer (km)	0.6215	mile (mi)
Volume		
cubic meter (m^3)	35.3134	cubic foot (ft^3)
cubic meter (m^3)	1.3077	cubic yard (yd^3)
cubic meter (m^3)	0.00081	acre-foot (acre-ft)
Flow rate		
cubic meter per second (m^3/s)	70.0771	acre-foot per day (acre-ft/d)
meter per second (m/s)	3.2808	foot per second (ft/s)
cubic meter per second (m^3/s)	35.3134	cubic foot per second (ft^3/s)
kilometer per hour (km/h)	0.6215	mile per hour (mi/h)

Aquatic Habitat Mapping with an Acoustic Doppler Current Profiler: Considerations for Data Quality

By David Gaeuman and Robert B. Jacobson

Abstract

When mounted on a boat or other moving platform, acoustic Doppler current profilers (ADCPs) can be used to map a wide range of ecologically significant phenomena, including measures of fluid shear, turbulence, vorticity, and near-bed sediment transport. However, the instrument movement necessary for mapping applications can generate significant errors, many of which have not been inadequately described. This report focuses on the mechanisms by which moving-platform errors are generated, and quantifies their magnitudes under typical habitat-mapping conditions. The potential for velocity errors caused by mis-alignment of the instrument's internal compass are widely recognized, but has not previously been quantified for moving instruments. Numerical analyses show that even relatively minor compass mis-alignments can produce significant velocity errors, depending on the ratio of absolute instrument velocity to the target velocity and on the relative directions of instrument and target motion. A maximum absolute instrument velocity of about 1 m/s is recommended for most mapping applications. Lower velocities are appropriate when making bed velocity measurements, an emerging application that makes use of ADCP bottom-tracking to measure the velocity of sediment particles at the bed. The mechanisms by which heterogeneities in the flow velocity field generate horizontal velocities errors are also quantified, and some basic limitations in the effectiveness of standard error-detection criteria for identifying these errors are described. Bed velocity measurements may be particularly vulnerable to errors caused by spatial variability in the sediment transport field.

Introduction

Physical habitat in lotic ecosystems is typically defined in terms of water depth, water flow velocity, and substrate composition. However, the combination of these three factors cannot provide a complete physical description of the conditions experienced by aquatic organisms. Other aspects of the physical environment, such as substrate stability or sediment particle impacts, may be equally important for some organisms. In addition, the spatial distribution of the various physical parameters may be significant. Lotic ecosystems consist of a continuum of physical conditions that can cover a wide range of depths, current velocities, and substrate materials. The attributes of a habitat patch therefore include its proximity to other habitat patches, the magnitudes of the environmental gradients within and between patches, and the spatial organization of patches at various scales (Townsend 1989; Poff and Ward 1990; Ward et al. 1999). Such attributes cannot be captured by isolated measurements at points. To achieve a landscape-scale understanding, individual measurements must be spatially referenced and compiled as a set of habitat maps depicting the spatial organization of the physical environment.

Compilation of a habitat map requires a large number of spatially-distributed measurements. In relatively large streams, most of the underwater environment is inaccessible and measurements must be obtained using remote sensing technologies. Acoustic depth finders are commonly used to obtain bathymetric data, and flow velocities can be determined by acoustic Doppler instruments. Several acoustic methods for sensing substrate composition are also available.

Acoustic Doppler current profilers (ADCPs) are especially useful for habitat mapping, because they are designed to simultaneously measure water velocities at multiple depths through most of the water column. When mounted on a boat with an integrated global positioning system (GPS), an ADCP provides a means for rapidly collecting 3-dimensional flow velocity data. ADCP data can be processed to yield a variety of ecologically-significant hydraulic parameters, and methods for extracting information regarding substrate stability from the ADCP data stream have been proposed (Rennie et al. 2002).

Because habitat mapping requires that ADCP data be collected from a moving boat, the data is potentially subject to errors caused by instrument motion. The potential for errors caused by mis-alignment of the by instrument's internal compass are widely recognized, but has not been quantified for moving instruments. Instrument movements can also generate a type of dynamic compass error that has not been previously documented. These dynamic errors can greatly exceed the errors typically expected from a well-calibrated compass, and are particularly troublesome when the velocity of the flow being measured is small. This report describes the mechanisms by which these types of errors are generated, and presents a quantitative analysis of their directions and magnitudes under typical habitat-mapping conditions.

Purpose and Scope

This report describes present capabilities for assessing physical habitat in aquatic ecosystems using data collected with a boat-mounted ADCP, and data quality issues that either have special relevance to this application or are inadequately documented elsewhere. It is not intended to provide a comprehensive discussion of ADCP operations and performance, many aspects of which are documented in literature supporting the use of ADCPs for stream gaging applications (e.g., Simpson 2001; Rehmel et al. 2003; Mueller 2003). Where descriptions of instrument characteristics are required to illustrate points not documented elsewhere, the discussion is based on a broadband Workhorse Rio Grande ADCP manufactured by RD Instruments, Inc.[1] Simpson (2001) provides additional details regarding the use of this instrument and the principles of its operation. However, the issues considered in this report are not instrument-specific, and most conclusions are applicable to ADCP data obtained with alternative instruments.

General Methods for ADCP Habitat Assessment

The approach to habitat assessment summarized below is based on the methods used by the River Studies Branch of the Columbia Environmental Research Center (CERC). Details concerning field methods and data processing methods used by CERC personnel can be found in Jacobson et al. (2002). It should be noted, however, that data collection and analysis procedures vary according to the circumstances and changes in equipment or software.

Most habitat mapping and assessment performed by CERC are conducted in the Lower Missouri River or its larger tributaries. The flow velocity field is sampled with either a 600-kHz or 1200-kHz RDI ADCP mounted off the side of a boat. In order to measure water velocities, the ADCP emits acoustic pulses, or pings, and records the echoes reflected back to the instrument by particles carried in the water column. The velocities of the particles reflecting the signal at various distances from the instruments are then calculated from shifts in the frequency (Doppler shift) and/or phase (time dilation) of the echoes (RD Instruments, Inc. 1996). The position and velocity of the instrument is determined with real-time kinematic (RTK) GPS. A precision echo-sounder or similar instrument is deployed simultaneously to collect additional bathymetric and substrate data.

---

[1] Trade names are used for information purposes only and do not constitute an endorsement by the U.S. Geological Survey.

Data Collection

Acoustic data are collected while driving the boat along pre-determined transects that the boat pilot can follow on a computer screen using commercial navigation software. Transects are normally oriented perpendicular to the direction of flow, in part because boat movement parallel to the flow direction tends to degrade data quality. High relative water velocities generated during upstream boat movement results in a high incidence of pings for which no data are recorded. We suspect that this data loss is related to the formation of bubbles or cavitations under the acoustic instruments. Downstream boat movement can lead to high absolute boat velocities, which amplify errors caused by slight mis-alignment of the instrument's internal compass. The effects of compass errors are described in detail in a later section of this report.

For most mapping applications, boat velocity is maintained at about 1-1.5 m/s, and the ADCP is configured to log ping data at a rate of one ensemble (an ensemble consists of all data for a water column vertical, and may be averaged over a group of pings) approximately every 2 seconds. This leads to a point spacing along each transect of about 1 ensemble every 2-3 m. The instrument is typically configured to average 6 pings for each ensemble, and to report water column velocities with a vertical spacing (bin size) of 0.25 m. These spatial parameters were selected to provide velocity-field data at a scale related to hydraulics and habitat use in the Missouri River. The implications of ping averaging and bin size on data accuracy are discussed later.

Transect spacing varies according to the spatial scale of the habitat being mapped. For reach-scale mapping, transects may be spaced as much as 100m apart (about 1/4 channel width in the Lower Missouri River). Mapping at this scale is generally intended to broadly quantify the availability of different habitat types within a reach (Fig. 1). A transect spacing of about 10m (1/40 channel width) is typical for meso-scale habitat assessment, such as mapping the depth and velocity fields over a single channel bar or in a single eddy (Fig. 2). Micro-scale habitat assessment consists of mapping features on the scale of individual bedforms, and requires a transect spacing of less than 5m (Fig. 3). Transect spacing for habitat assessment in most streams would clearly be much smaller than those used on the Lower Missouri River, which is among the largest rivers in the nation.

Data Processing

Processing of the ADCP data begins with exporting the velocity data from the ADCP system software into an ASCII format that can be manipulated using text handling scripts. Standard processing includes calculation of depth-averaged velocities for each ensemble, and the extraction of discrete horizontal or vertical planes in the 3-dimensional data set for further analysis. Two-dimensional data are gridded using commercially-available kriging algorithms, and the gridded data are imported into a geographic information system (GIS) for map production and analysis.

A variety of derivative data products can be created from ADCP velocity data and combinations of velocity data with other measurements. For example, maps showing the spatial distribution of Froude number, which is sometimes used as an index of habitat suitability (Jowett 1993), can be readily constructed by combining flow depth with flow velocity. Shear and turbulence may also be of ecological interest. Associations between certain organisms and areas with strong velocity gradients can be evaluated in a GIS (Fig. 4), and other more sophisticated analyses of turbulence and flow vorticity have been proposed (Shields et al. 2003).

New Techniques for Assessing Benthic Habitat

Recent work at CERC includes the development of methods utilizing the ADCP's bottom-track capability to assess environmental conditions at the stream bed. Bottom-tracking refers to a method normally used to determine ADCP velocity when GPS positioning is not available. It consists of acoustic pings whose echoes return information regarding the velocity of bed motion with respect to the instrument. Bottom-track pings are distinct from the pings used to measure water velocities, and have somewhat different characteristics. If the bed is assumed to be stationary with respect to the Earth, the bottom-track velocity vector is equal in magnitude to the velocity magnitude of the instrument, but in an opposite direction. Thus the velocity and direction of movement of the instrument can be determined while moving through a stream cross section during a discharge measurement.
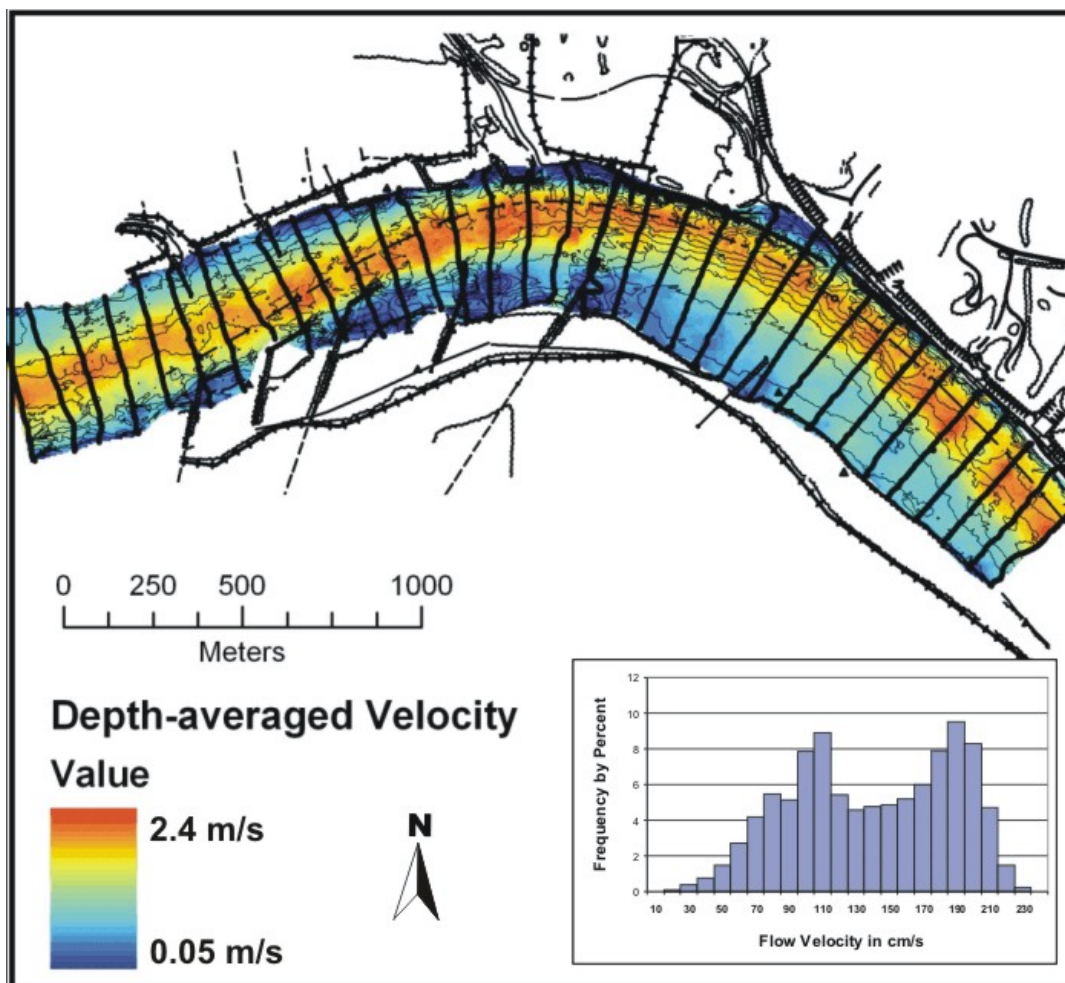
Figure 1. Reach-scale map of depth-averaged velocity in the Lower Missouri River near Rocheport, MO, on May 28, 2004. Water discharge at the time was 143,000 ft³/s. Black lines perpendicular to the channel are data transects with 100m spacing. Channel boundaries, dikes, and depth contours are also shown in black.

However, in cases where sediment is moving on or near the stream bed, bottom-track velocities are not representative of instrument velocity because the particle velocity information is incorporated into the bottom-track echoes and interpreted by the instrument as bed motion. Such apparent bed motion due to moving particles near the bed is independent of any instrument motion. Standard stream gaging protocols (US Geological Survey 2001) include tests to detect bed sediment motion, or moving-bed conditions. Where the bed is found to be in motion, it may be necessary to track ADCP motion using GPS, or compute discharge from velocity profiles measured at stationary verticals. The moving-bed velocity itself can be isolated if the instrument is held stationary, or all actual instrument motion is subtracted from the apparent instrument motion determined from the bottom-track measurements. When isolated in this manner, the moving-bed velocity is useful for evaluating flow velocities very near the stream bed and for quantifying the movement of bed materials.

Sampling of bedload transport rates in conjunction with ADCP data suggest that bed velocities measured with a 600-kHz broadband ADCP are indicative of sediment bedload transport rates near the bed (Fig. 5). Rennie et al. (2002) previously documented a correspondence between sediment transport and bed velocity measured with a different type of acoustic Doppler instrument. Substrate motion has a direct impact on benthic organisms, many of which require a stable surface on which to maintain their positions. Intense transport of bed sediments probably also constitutes an environmental hardship for other species, such as benthic fishes, and the ability to detect sediment motion at the bed has potential for verifying and improving the accuracy of substrate classification techniques.
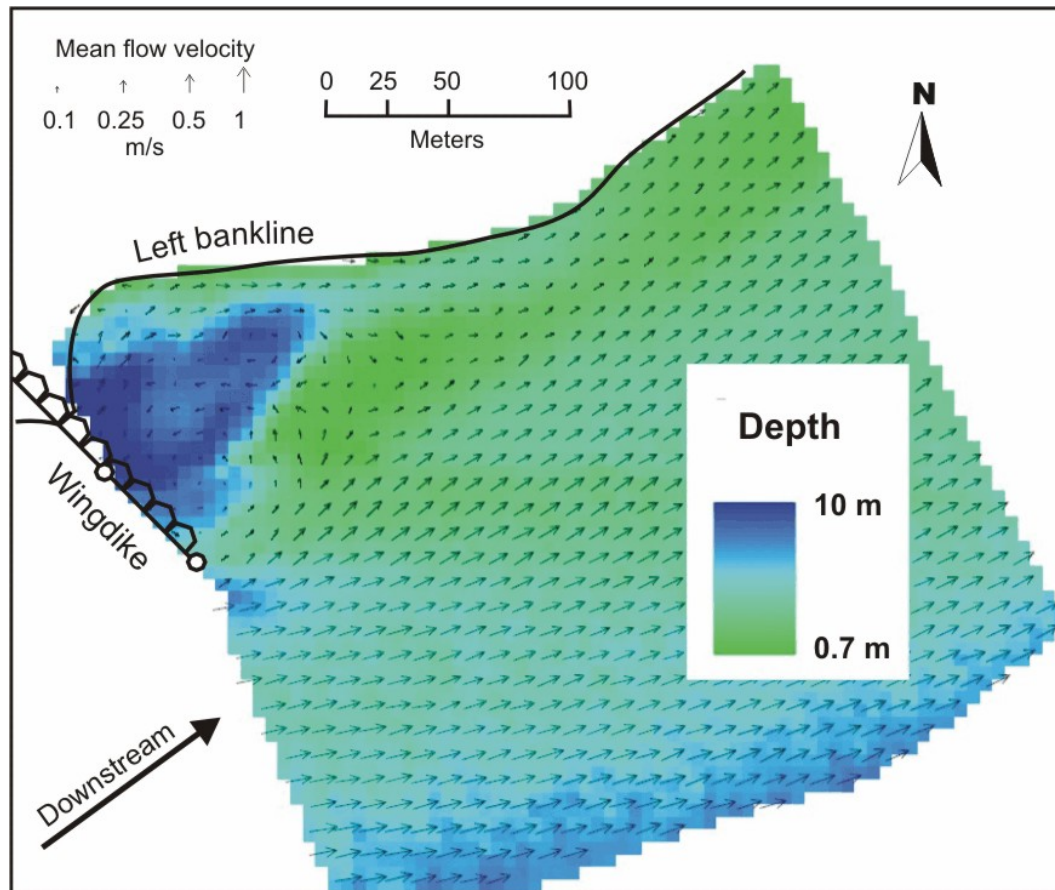
Figure 2. Meso-scale map showing 2-dimensional velocity field and bathymetry in an eddy downstream from a wing dike structure near Miami, MO. Proportional arrows showing depth-averaged velocity distribution are gridded at 10 m resolution from ADCP data collected on transects spaced 10 m apart.

Comparison between bed velocity measurements and the vertical velocity distribution in the water column also show that high bed velocities are indicative of water flow velocities within several cm from the bed (Fig. 6). Conventional ADCP measurements are incapable of accurately measuring water velocities closer to the bed than about 6-14% of the distance between the ADCP and the bed (h_d). Because the acoustic beams emitted by ADCPs are pointed at an angle (β) from vertical, acoustic echoes from the water column less than ($h_d - h_d\cos\beta$) in height above the bed are contaminated with echoes from the bed (RD Instruments, Inc. 1996). The broadband ADCPs used at CERC have $\beta = 20°$, whereas some other instruments have $\beta = 30°$. Under moving bed conditions, the use of bottom-tracking to calculate bed velocities allows water velocities to be estimated much nearer the bed than is possible using conventional ADCP measurements.

When made spatially explicit through mapping, bottom-track bed velocities can be used to define the distributions of stable or unstable substrates, the severity of sediment particle bombardment, and near-bed water velocities at scales ranging from the river reach (Fig. 7) to individual bedforms (Fig. 3). The full ecological implications and applications of this new technique have not yet been fully explored. Although the method is potentially promising for investigating both biological and physical aspects of the benthic environment, its utility depends in large measure on the proper recognition of its limitation and potential for error. As discussed below, bed velocity measurements are substantially more sensitive to several sources of error than are water column velocity measurements.
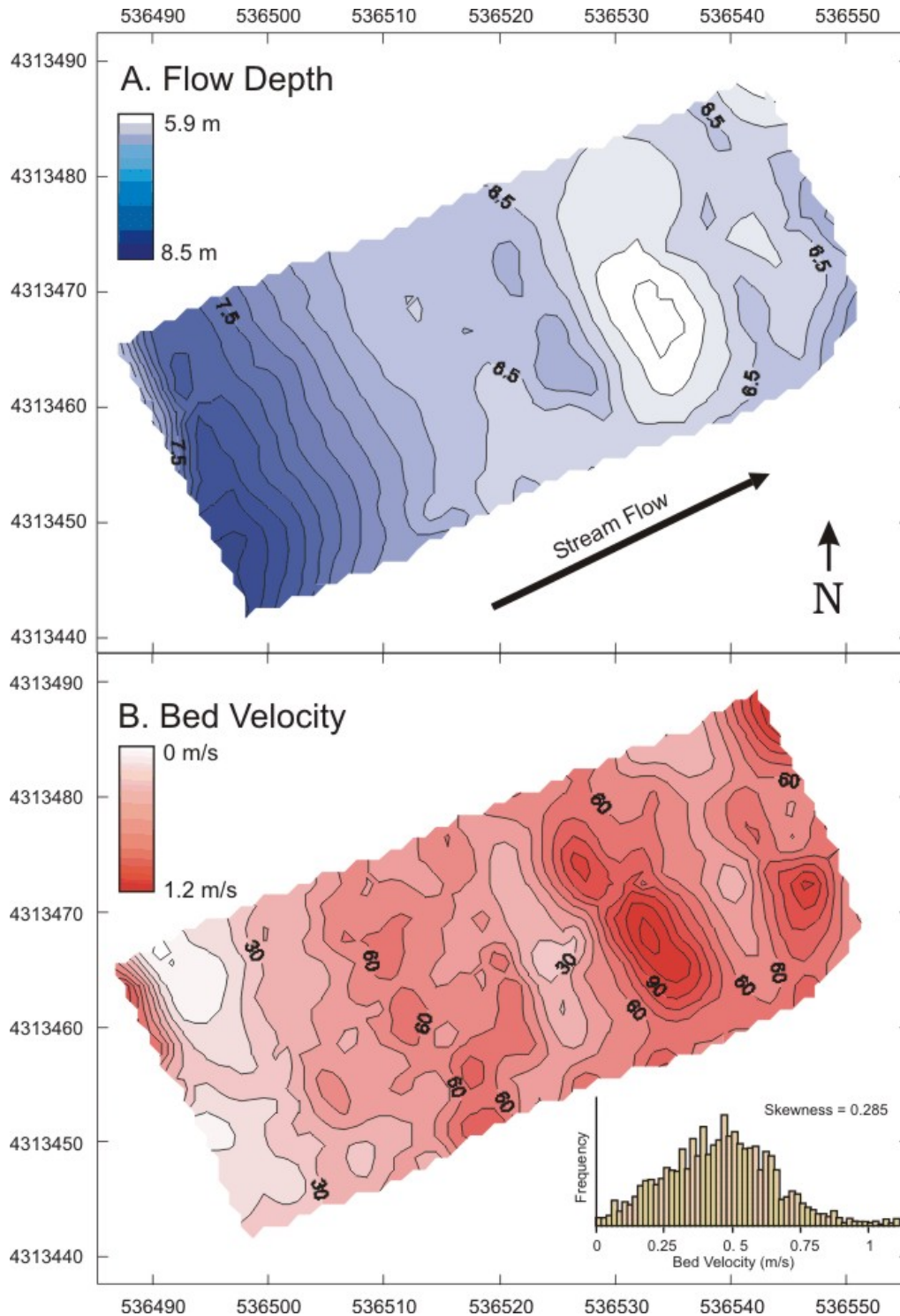
Figure 3. Micro-scale maps showing A) bed topography and B) the distribution of bed velocity over a single dune. Bed velocity was calculated by subtracting instrument velocities determined by GPS from ADCP bottom-track velocities collected on 3m transects. Zones of higher bed velocities correspond with higher parts of the bed. Discharge at the time was 3,964 m^3/s.
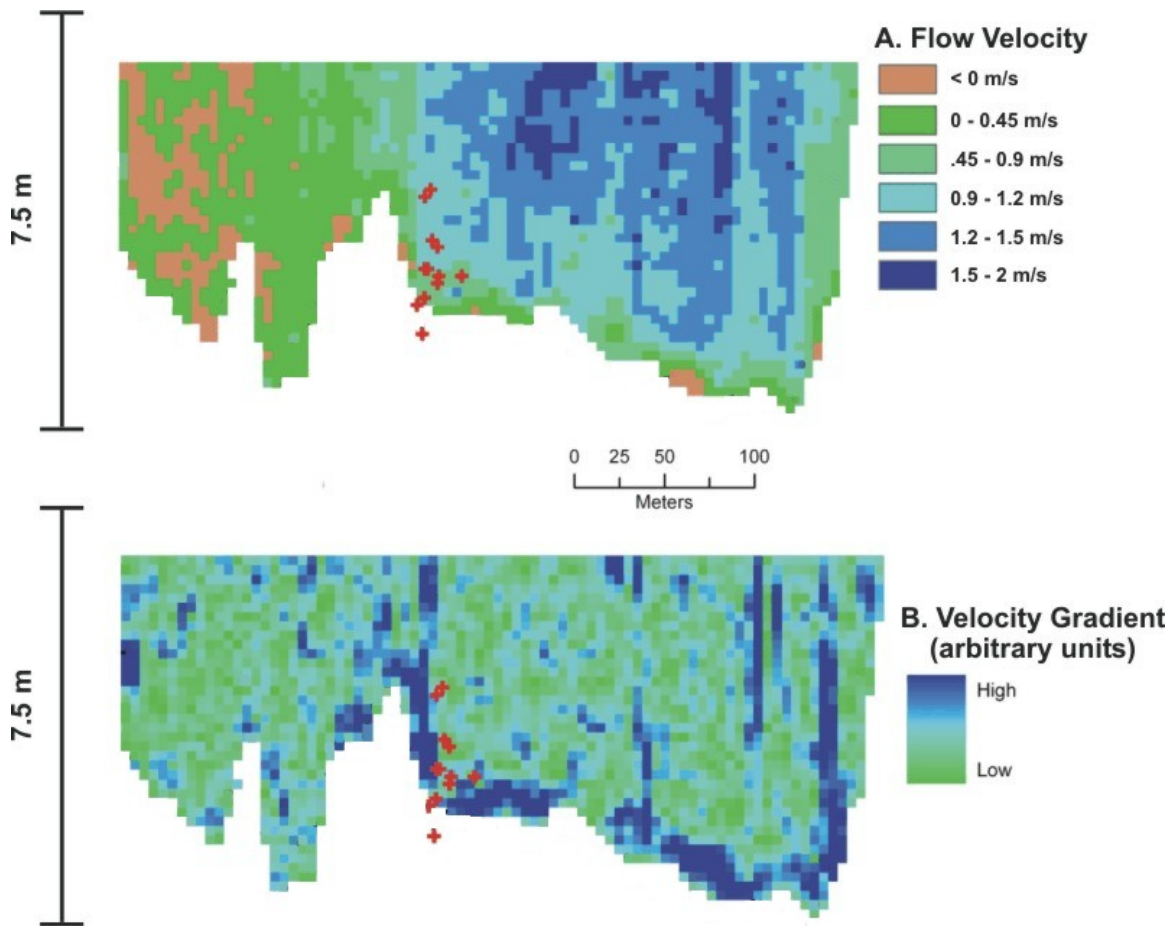
Figure 4. Downstream velocity and velocity gradient distributions at a cross section near Huntsdale, MO. Points where a Pallid sturgeon was located on several occasions by telemetry crews are indicated with red crosses. Fish locations are associated with A) flow velocities of about 1 m/s and B) high velocity gradients.
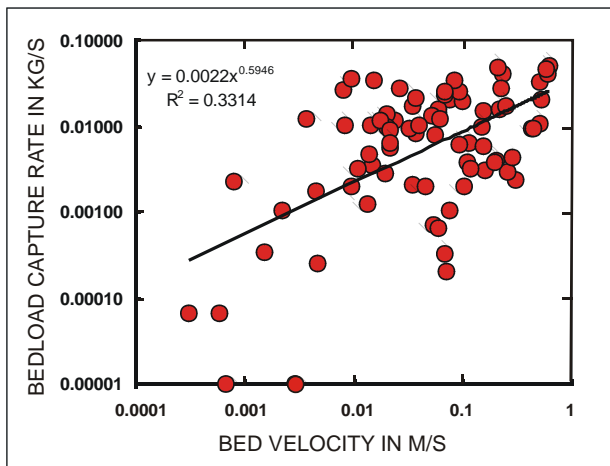
Figure 5. Graph showing bedload capture rate versus bed velocity. Bedload capture rates were determined from samples taken with a Helley-Smith bedload sampler while recording ADCP bottom-track data with integrated RTK GPS. Bedload capture rates increase when bed velocity is greater than about 0.1 m/s.

7
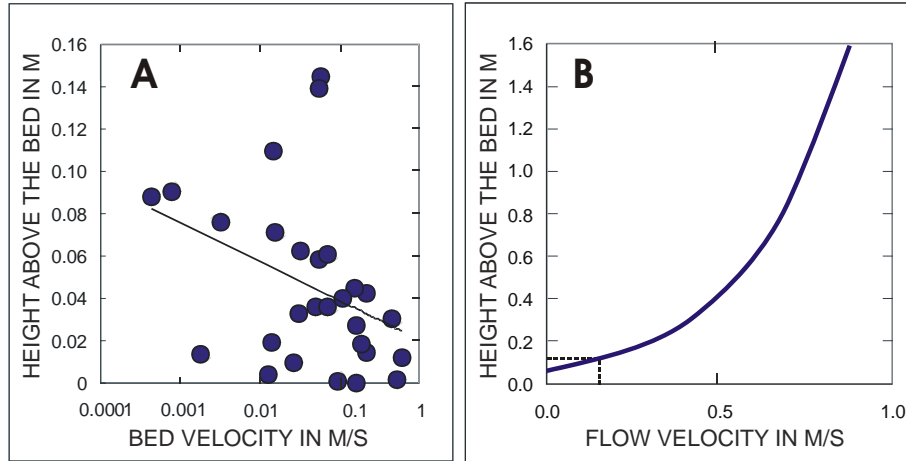
Figure 6. A) Graph showing the height above the bed where water flow velocities are equal to the bed velocity. Bed velocity corresponds to water velocity within several cm of the bed, especially for higher bed velocities. Water flow velocities near the bed were estimated from ADCP velocity profile data collected through most of the water column. B) Graph of a near-bed water velocity profile illustrating the height above the bed where the flow velocity equals the measured bed velocity. The velocity profile was constructed from flow velocity data collected at a point where the bed velocity was about 0.21 m/s. The flow velocity equal to the bed velocity occurred at a height of about 0.12 m above the bed.
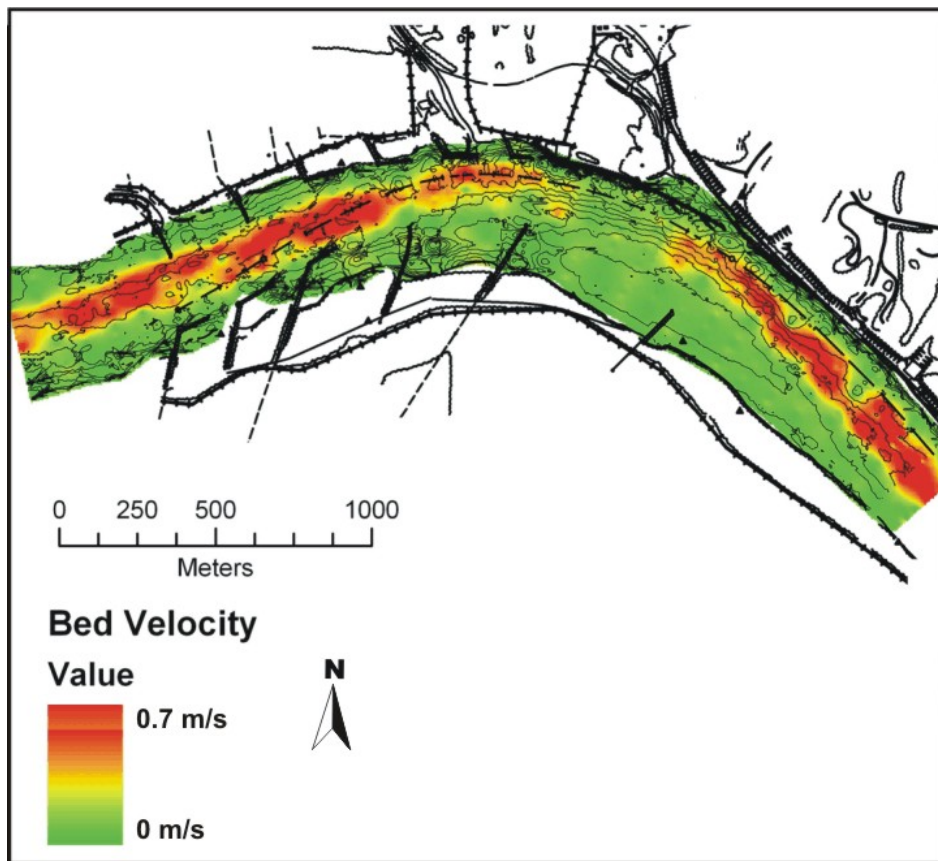
Figure 7. Reach-scale map of bed velocity in the Lower Missouri River near Rocheport, MO, on May 28, 2004. Bed velocity was calculated by subtracting instrument velocities determined by GPS from ADCP bottom-track velocities. Channel boundaries, dikes, and depth contours are shown in black. Bedload sampling conducted on the same day confirmed that thalweg bedload transport rates were anomalously low near the bend apex. Both an acoustic substrate classification system and physical sampling indicated that the bed was locally scoured to gravel or bedrock in that location.

8

General Aspects of ADCP Data Quality

ADCP measurements are subject to numerous errors and uncertainties, some of which are amplified or generated by motion of the instrument during data collection. Because the use of a mobile platform is essential for mapping habitat in large rivers, the following discussion focuses on the characteristics of errors related to instrument motion. Errors that are inherent to instrument operation without regard to instrument motion are described at length elsewhere (Rennie et al. 2002; Simpson 2001), and will only be briefly summarized here.

Instrument Noise

All ADCP data includes random errors associated with the instrument's internal electronics. Simpson (2001) describes the physical principles involved with the generation of instrument noise in broadband ADCPs. In general, the standard deviation of random errors in individual velocity measurements caused by instrument noise increases with decreasing bin size and decreasing instrument frequency. Information regarding the magnitude of instrument noise for various instruments is available from the equipment manufacturers.

Because these types of errors are randomly distributed, they are typically dealt with by averaging a large number of individual measurements. The standard error of n averaged measurements is equal to the standard deviation of the individual errors divided by the square root of n (RD Instruments, Inc. 1996). The standard deviation of the instrument errors for velocity measured in a 25-cm water column bin using a single ping from a 1200 kHz broadband ADCP using default configurations is ±0.129 m/s. For ensembles consisting of 6 pings averaged together, the precision of the velocity measurements is described by a standard error of ± 0.053 m/s. Subsequent gridding of the ensembles for map production results in additional data averaging and further error reduction (Rennie and Millar 2004).

Velocity Ambiguity Errors

Velocity ambiguity errors are potentially large errors that can occur when stream flow velocities are large relative to the instrument velocity. For an explanation of these errors, the reader is again referred to Simpson (2001). Stream gaging protocols may discourage data averaging within ensembles, so that the un-averaged data can be inspected and velocity ambiguity errors can be identified. The magnitude of the instrument velocity relative to the water required to produce ambiguity errors depends on an adjustable radial ambiguity velocity threshold, which for a Rio Grande ADCP operating in the standard mode (water mode 1) has a default value of 1.7 m/s. This threshold corresponds to a horizontal relative water velocity of about 3.3 m/s [see equation (3.1) in Simpson (2001)]. The potential for velocity ambiguity errors to affect habitat mapping is therefore small if upstream instrument movement is avoided, and absolute velocities of the instrument platform are low. The ambiguity velocity threshold can be increased for conditions in which relative water velocities of 3.3 m/s or more cannot be avoided, although increasing the threshold does increase the single ping standard deviation.

Bottom-tracking and GPS Errors

The effect of instrument noise on bottom-track pings is much smaller than for water-column pings. The length of bottom-track pings is much larger than the water column bin size, so that bottom-track pings contain more acoustic energy than water column pings, and the bed reflects more of the ping energy than particles suspended in the water column do. Thus, the bottom-track echoes from the bed are much stronger than the echoes of water-column pings from the water column, so that bottom-track errors due to instrument noise are negligible (RD Instruments, Inc. 1996).

However, as described above, sediment motion near the bed can interfere with bottom-tracking as a means for tracking instrument motion. Instrument positioning must then be accomplished by GPS, whereas the bottom-tracking 'errors' themselves can be exploited to estimate sediment and fluid velocities at the bed. Rennie et al. (2002) empirically found that differentially-corrected GPS errors result in average velocity measurement errors of

about 0.007 m/s. Habitat mapping with RTK GPS, which has horizontal and vertical precision on the order of a few cm, virtually eliminates GPS errors.

Spatial Averaging

The spatial averaging inherent in ADCP operation contributes to uncertainties in both the magnitude and position of the recorded data. Each of several transducers in an ADCP emit an acoustic beam that spreads as it propagates away from the instrument. The area ensonified by each beam therefore increases with distance from the instrument. The rate of the increase is specified in terms of beam width, that is, the angle at which the width of the region where the sound pressure is at least half its value at the center of the beam increases with distance from the transducer (Fig. 8). Beam width in radians (ϕ_b) for a given transducer is a function of acoustic wavelength (λ) and transducer diameter (d), according to $\phi_b = 4\lambda/(2^{0.5}\pi d)$ (Deines, undated). Beam widths are between 1° and 2° for both the 600 kHz and 1200 kHz Rio Grande ADCPs.

Each of the beams is angled away from the vertical axis of the instrument, so that the horizontal distance between the areas insonified by the beams also increases with increasing depth below the instrument. Four-beam ADCPs make use of orthogonal pairs of beams, where the beams in each pair are angled in opposing horizontal directions, ie, a left-looking and right-looking pair and a forward-looking and backward-looking pair. In any horizontal plane below the instrument, the distance between the center of the ensonified areas and the point directly under the instrument is equal to [$h_d \tan(\beta)$], where h_d is the flow depth minus the instrument draft and β is the angle of the acoustic beam from vertical (Fig. 8). The 4 beams emitted by our ADCPs are each oriented at a 20° angle away from the vertical axis, so that, if h_d over a portion of the stream bed were 6m, the bed velocity at the point directly under the ADCP would be calculated from bed velocity components in 4 separate regions of the bed located on the perimeter of a circle with a diameter of [$2 \cdot 6 \cdot \tan(20°)$] ≈ 4.4 m. There can be no assurance that measurements in the 4 perimeter areas are representative of velocity at the center of the circle.

For some applications it may be necessary to avoid overlap in the areas sampled by adjacent ensembles. For example, Shields et al. (2003) indicate that their approach for measuring flow vorticity, i.e., the degree of rotational motion in the stream flow, requires that individual velocity measurements be statistically independent and separated by a constant distance. Shield et al. (2003) suggested that individual ensembles be thinned to a spacing of [$2h_{dmax} \tan(\beta)$], where h_{dmax} indicates the maximum observed value of h_d.
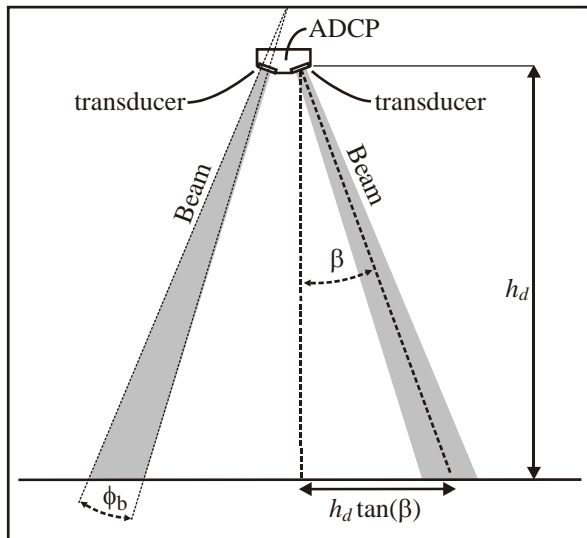

Figure 8. Diagram illustrating change in the distances between the regions ensonified by different ADCP beams and the change in the cross sectional area of the beams with distance from the instrument. The distance between the centers of two opposing beams is $2h_d\tan(\beta)$, where the distance between the transducer centers is neglected.

Compass Errors

The velocity information carried in the acoustic signals recorded by an ADCP indicates the velocity of the target fluid or surface relative to the ADCP's internal compass. Because the compass is affected by various sources of error, including changes in magnetic declination, the presence of near-by ferrous objects, magnetic fields generated by instrument electronics, and instrument accelerations, it is unlikely to be perfectly accurate. Where the instrument velocity vector is determined by GPS, the azimuth of the instrument motion is relative to geographic coordinates, whereas the azimuth of the velocity vector is relative to the ADCP's internal compass. Subtracting velocities determined by GPS from velocities determined by the ADCP generates errors in both the absolute magnitudes and azimuths of measured fluid or sediment velocities.

The following discussion requires terminology for distinguishing between instrument motion and the motion of the objects whose velocity is being measured. For water column measurements, the physical object of interest is a volume of flowing water. In the case of bottom-track measurements, the object of interest is the layer of moving bed material in an area of the stream bed. We use the general term "target" to refer to either type of object.

Compass Calibration Errors

Compass calibration error refers to a persistent misalignment between true geographic north and compass north. The angle between geographic north and compass north is here designated by α, with positive α referring to a counterclockwise rotation from true north. The magnitude of α depends on the quality of calibration procedures used to correct for compass misalignments. The calibration procedure consists of two parts: determining the correct magnetic declination for the field site and entering it in the system software, and correcting for one-cycle magnetic errors related to instrument electronics and magnetic objects in the instrument's vicinity. Although the correct magnetic declination for the site can be estimated in the field using the ADCP compass and system software, we recommend obtaining accurate declination values from an updated chart or on-line from the National Geophysical Data Center (NGDC). Declinations for any field site can be computed by entering latitude and longitude coordinates for the site into the NGDC utility at http://www.ngdc.noaa.gov/seg/ geomag/jsp/Declination.jsp. One-cycle errors are corrected in the field using procedures specified by the equipment manufacturer. Compass calibration instructions for our instrument (WinRiver version 10.05, RD Instruments, Inc.) specify that the total compass error should be less than ±5°, and describe an example one-cycle calibration resulting in a total residual compass error of ±0.84°. As demonstrated below, a 5° error is unacceptable for mapping applications. Fortunately, experience indicates that calibrations accurate to less than ±0.5° degrees are often possible.

In addition to the magnitude of α, the severity of the velocity errors resulting from a compass misalignment depends on the velocity of the instrument relative to the velocity of the target, and the direction the instrument is moving relative to the direction the target is moving. Joyce (1989) presented equations describing the impact of compass misalignments on ADCP velocity measurements as part of the development of a compass calibration procedure. However, the equations for computing velocity component errors do not include the velocity of the instrument (see equations (14) and (15) in Joyce 1989), and do not correctly account for the effects of instrument motion.

The geometry of the interactions between instrument movement and compass misalignment is illustrated in Fig. 9. A northward instrument motion relative to geographic coordinates is shown by the longer solid arrow labeled (1) in Fig. 9a, and the corresponding apparent motion of the target is indicated by the south-pointing dotted arrow (2). The actual target velocity in geographic coordinates is indicated by shorter solid arrow (3). The total apparent target motion is defined by a vector (not shown) from the origin to point G_1. When the actual instrument motion is subtracted from point G_1, as indicated by the long grey arrow labeled (4), the resulting target velocity vector (5) from the origin to point G_2 is equal to the actual target velocity.

However, if the instrument's compass coordinate system is rotated relative to the geographic coordinate system by an angle α, the instrument velocity vector, the apparent target velocity vector caused by instrument motion, and the actual target velocity vector are all rotated by α, as indicated by arrows (6), (7), and (8). The actual instrument movement remains in geographic coordinates. Subtraction of this instrument movement from the sum of the two rotated vectors is indicated by the long grey arrow labeled (9). The apparent target velocity vector resulting from these real and apparent motions is the vector from the origin to point P, as indicated by the black dashed arrow

11

(10). This arrow is clearly longer than the actual target velocity (3). The azimuths of the two arrows are different as well. Fig. 9b illustrates a similar situation, except that the direction of the actual target velocity is reversed. In this case, the compass misalignment generates a near reversal in the azimuth of the measured target velocity vector as well as a large error in its magnitude.
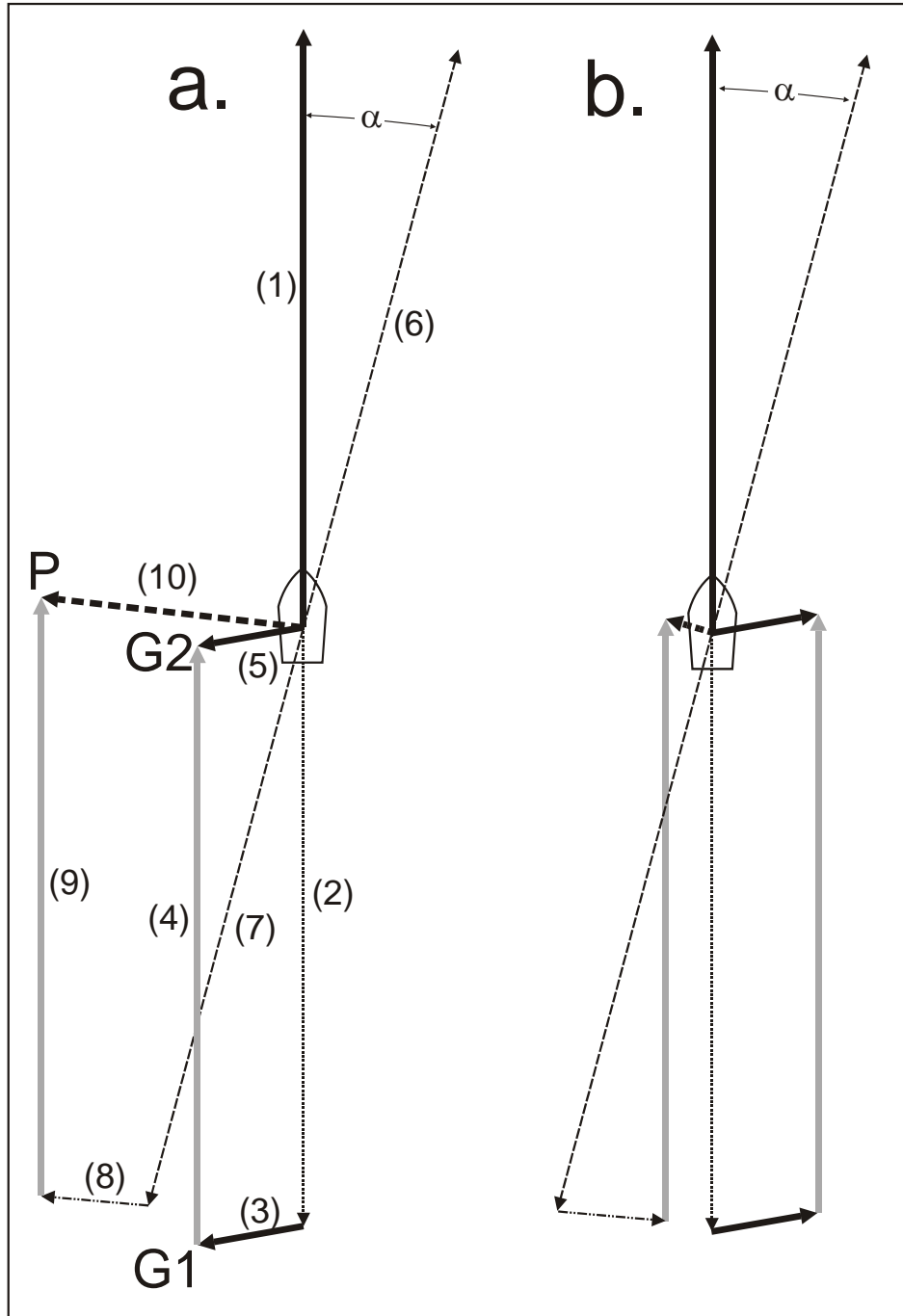
Figure 9. Diagram illustrating how ADCP compass errors generate velocity errors. See the text for explanation. The symbol at the vector origin represents a boat.

We numerically evaluated the errors corresponding to different combinations of compass error, instrument velocity magnitude, target velocity magnitude, and relative azimuth of instrument and target velocities. Instrument velocity vectors were arbitrarily assumed to have an origin at 0,0 and a constant azimuth of 0, while all other

variables were systematically varied. The coordinates of the terminus of the rotated vector representing the apparent target velocity due to instrument velocity, (7) in Fig. 9, are:

$$X_7 = -V_G \sin(\alpha); \qquad \text{(1a)}$$

$$Y_7 = -V_G \cos(\alpha) \qquad \text{(1b)}$$

where V_G is the actual instrument velocity according to GPS and X and Y coordinates are in units of velocity (m/s). The coordinates of the terminus of the rotated apparent target velocity vector, i.e., arrow (8) in Fig. 9, are:

$$X_8 = X_7 + V_T \sin(\beta); \qquad \text{(2a)}$$

$$Y_8 = Y_7 + V_T \cos(\beta) \qquad \text{(2b)}$$

where V_T is the true target velocity, $\beta = \phi + \alpha$, and ϕ is the true azimuth of the target velocity vector relative to the direction of instrument motion. The coordinates of point P, which designates the vector sum of apparent target movements in instrument coordinates minus true instrument movement are:

$$X_P = X_8; \qquad \text{(3a)}$$

$$Y_P = Y_8 + V_G \qquad \text{(3b)}$$

The vector from the origin to point P represents the apparent target velocity, the magnitude and azimuth of which are readily obtained from the coordinates of P. The magnitude of the apparent target velocity vector is denoted by V_A, and the magnitude of error contained in V_A is given by $(V_A - V_T)$.

This numerical analysis shows that relatively small compass errors can result in significant target velocity errors, depending on the values of the other variables. A compass error (α) of 1° can produce errors of up to 50% in V_A if the true instrument velocity (V_G) is 30 times greater than the true target velocity (V_T) and the relative angle between the instrument and target velocities (ϕ) is near 90° or 270° (Fig. 10). Errors approaching 20% can still occur when V_G/V_T is 10, such as a when boat velocity is 1 m/s and target velocity is 0.1 m/s.

Compass errors can also produce severe errors in the measured target velocity azimuths (azimuth error is here defined as ($\Phi - \phi$), where Φ is the apparent azimuth of target motion). For example, a compass error of 1° can result in maximum azimuth errors ranging from about 10° when V_G/V_T is 10, to about 30° when V_G/V_T is 30 (Fig. 11). The azimuth errors realized for a given α and V_G/V_T are near zero when ϕ is near 90° or 270°, but increase rapidly as ϕ deviates from those values. Error maxima occur near $\phi = 0°$ and $\phi = 180°$ for small V_G/V_T, and for progressively larger values of ϕ as V_G/V_T increases.

Because the magnitude of velocity errors caused by compass misalignment depends on the ratio of the instrument velocity to the target velocity, the impact of compass errors is particularly important when target velocities are low. Boat velocities should therefore be minimized when mapping in low velocity areas, such as eddies or backwaters, and when mapping bed velocities. Significant errors in measurements of high velocity targets can also occur if boat speeds are excessive. For example, errors in even high velocity flows are likely if mapping is conducted while traveling downstream under power. Because downstream mapping adds the surface current velocity to any powered boat velocity, the net boat velocity is certain to be equal to or greater than the surface flow velocity, and will probably be considerably greater than the flow velocity at depth. ϕ is probably near zero under such circumstances, a configuration that is relatively resistant to errors in the velocity magnitude but very susceptible to azimuth errors (see Figs. 10, 11). The resulting compass errors are therefore easily identified by the presence of measured velocity vectors that are oblique to the general flow direction.
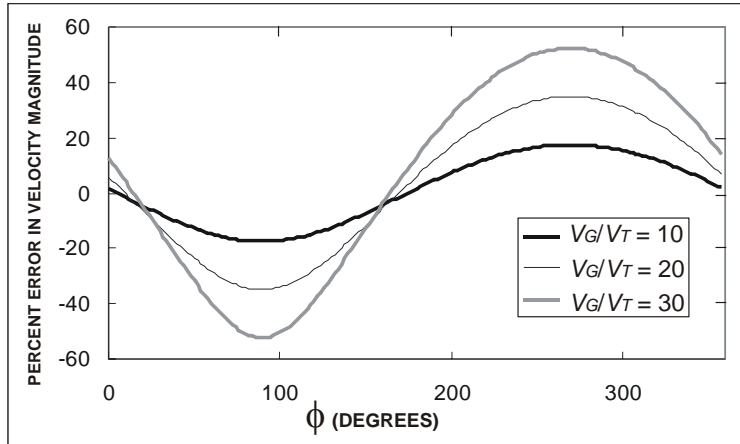
Figure 10. Graph showing the variation in the percent error in the magnitude of ADCP velocity measurements for a 1° compass error. Errors are a function of the angle between the directions of instrument movement and stream flow or bottom-track movement (ϕ), and the ratio of the instrument velocity determined from GPS (V_G) and the velocity of the target being measured (V_T).
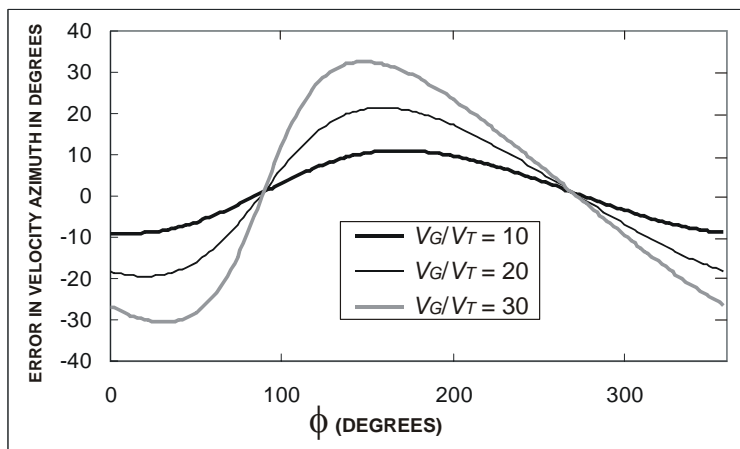

Figure 11. Graph showing the variation in the error in the azimuth of ADCP velocity measurements for a 1° compass error. Errors are a function of the angle between the directions of instrument movement and stream flow or bottom-track movement (ϕ), and the ratio of the instrument velocity determined from GPS (V_G) and the velocity of the target being measured (V_T).

The situation is reversed when instrument motion is approximately perpendicular to the current, as is the case for most mapping applications. Azimuth errors are small when flow is perpendicular to the instrument velocity, even when the magnitudes of the errors are large. Consequently, data containing substantial errors can appear to be valid. In stream gaging, bias caused by compass misalignment can be controlled by traversing stream transects in opposite directions and averaging the discharge results (US Geological Survey 2001). A compass calibration error that causes the velocity of a perpendicular flow to be exaggerated in one direction of traverse will cause the velocity to be underestimated when the transect is traversed in the opposite direction. This solution is generally not practical for mapping applications.

Dynamic Compass Errors

Dynamic compass errors refer to compass fluctuations caused by instrument accelerations that physically displace movable parts within the instrument compass. The angular errors in compass readings caused by dynamic forces acting on the compass can be much larger than typical compass calibration errors, and the corresponding velocity errors are potentially large. As with compass calibration errors, the magnitude of the resulting velocity error is a function of the absolute boat velocity. But in the case of dynamic compass errors, boat motions can also generate accelerations, and thus also produce angular errors in the compass heading. We first noted the effects of dynamic compass errors in bed velocity data mapped under conditions of relatively low bedload transport. Measured bed velocities were noticeably greater at the edges of the mapping area where the boat turned to make another pass (Fig. 12). Experimental results have since confirmed that acceleration, such as would occur when bringing the boat about, cause compass anomalies. The effect can be readily observed by shaking an ADCP whose

14

heading is fixed while logging data. We produced instantaneous heading errors of up to 9° in a fixed ADCP by rattling the aluminum mount connecting the instrument to a parked boat.
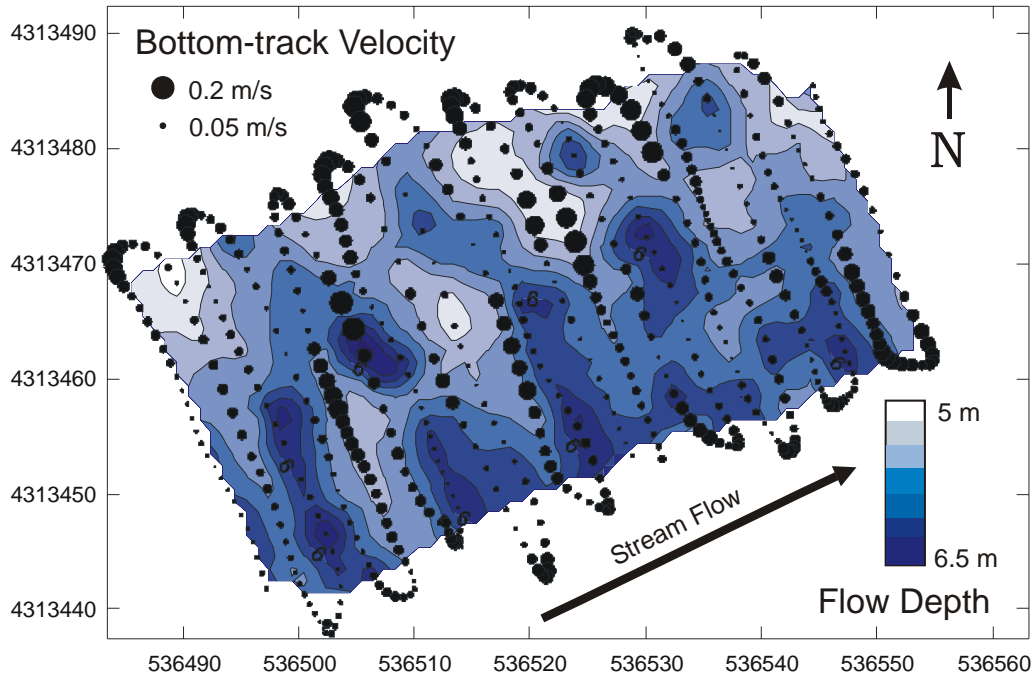

Figure 12. Micro-scale map showing bed topography and bed velocity errors cause by instrument accelerations. Black dots are proportional to a 5-ping moving average of the measured bed velocity magnitudes. The boat path during data collection corresponds with the trail of dots, starting at the lower left corner of the mapped area and ending at the upper right. Bed velocity magnitudes are consistently large at the ends of transects where the boat turned to make another pass. Area shown is the same location shown in Figure 3, but at much lower discharge (2,942 m³/s).

Some dynamic heading errors are positive in sign, whereas others are negative. If the orientation of the boat velocity vector and the target velocity vector are such that a positive heading error produces a positive velocity error, then a negative heading error will produce a negative velocity error. For transects oriented perpendicular to the flow direction ($\phi \sim 90°$ or $270°$), the magnitudes of velocity errors caused by positive and negative heading errors are nearly equal, and the errors could cancel out if a sufficient number of ensembles with both positive and negative heading errors were averaged together. However, error magnitudes become noticeably asymmetric when V_G/V_T is large (Fig. 13), so that the sum of the velocity errors from two equal but opposite heading errors is not zero in general. Limited field tests conducted by us suggest that ensemble averaging substantially reduces the effects of dynamic compass errors, but further study is needed to determine the magnitude of the residual errors.
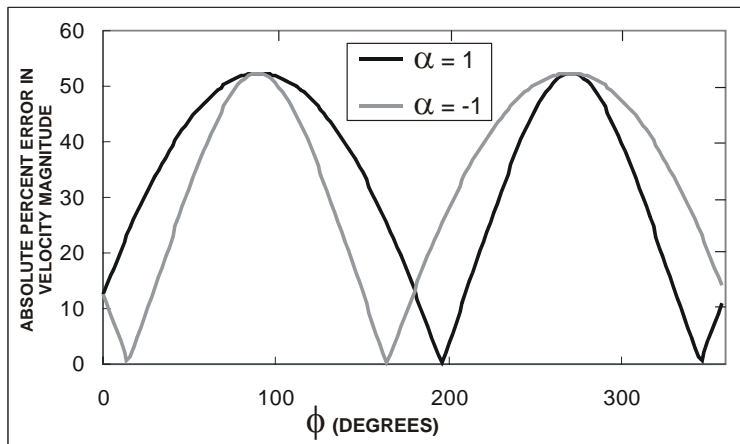

Figure 13. Graph showing the variation in the absolute value of the percent error in the magnitude of ADCP velocity measurements for $V_G/V_T = 30$ and compass errors of 1° and ●1°. Asymmetry in the error distributions are 180° out of phase for positive and negative α.

15

Errors Caused by Heterogeneous Velocity Field

Each beam of an ADCP can measure only the component of target velocity that is parallel to the beam. Horizontal and vertical components of the target velocity are computed from the beam-parallel components using equations that require the assumption that the velocity field is spatially homogeneous over the domain sampled by all ADCP beams. Rennie et al. (2002) presents the system of equations used to compute velocities for 3-beam instruments, whereas 4-beam systems are discussed below.

In 4-beam ADCPs, each pair of opposing beams is used to compute a horizontal velocity component in the vertical plane containing the pair, as well as a vertical velocity component. Because the velocity components computed by each beam pair are independent of the velocity components computed by the other beam pair, error generation can be evaluated by considering a single pair. Fig. 14 illustrates how the horizontal and vertical velocity components can be derived from these pairs of beam-parallel components.
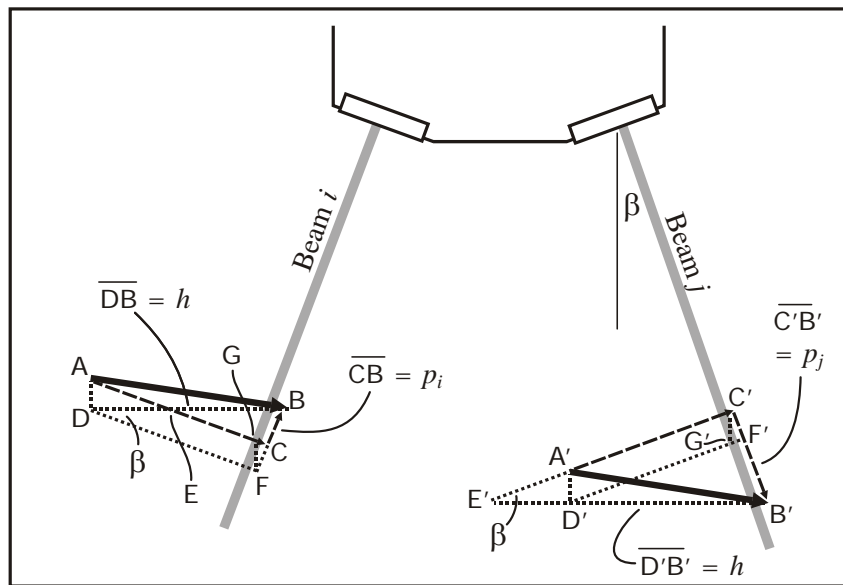

Figure 14. Diagram illustrating a pair of opposing acoustic beams and the geometric relations use to compute the horizontal and vertical velocity components from the beam parallel components. See the text for explanation.

The solution requires the assumption that the velocity field at any given distance from the instrument is spatially homogeneous. Flow velocity vectors of equal magnitude and direction approaching two opposite beams (segments AB and A'B') have beam parallel components (p_i and p_j), which are represented on Fig. 14 by segments CB and C'B'. Positive vectors are defined to point up and to the right, such that p_i is positive and p_j is negative. The flow velocity vectors also have horizontal (segments DB and D'B') and vertical components (w_i and w_j) represented by segments AD and A'D'. Beam-parallel components CB and C'B' could also be generated by horizontal flow vectors indicated by segments EB and E'B'. EB is equivalent to (DB−DE), and its length is given by $p_i/\sin(\beta)$. E'B' is equivalent to (D'B'+D'E') and its length is given by $-p_j/\sin(\beta)$. Triangles ADE and A'D'E' are identical, so segments DE and D'E' are equal in length. The length of the true horizontal velocity components (DB = D'B' = h) are therefore equal to the mean length of EB and E'B', which is given by:

$$h = (p_i - p_j)/2\sin(\beta) \qquad\qquad (4)$$

The measured value of p_i is the sum of the beam-parallel component of h (equal to FB = $h\sin(\beta)$) and the beam-parallel component of the flow velocity vector (CF). Likewise, p_j is the sum of the beam-parallel component of h (equal to F'B' = $-h\sin(\beta)$) and the beam-parallel component of the flow velocity vector (C'F'). Thus:

$$CF = p_i - h\sin(\beta) \qquad\qquad (5a)$$

$$C'F' = p_j + h\sin(\beta) \qquad\qquad (5b)$$

GF and C'G' are equivalent to AD and A'D', and so also represent the vertical components of the flow velocity vectors. The vertical components are therefore given by:

$$w_i = CF/\cos(\beta) \qquad\qquad (6a)$$

$$w_j = C'F'/\cos(\beta) \qquad\qquad (6b)$$

Substituting (4) and (5) into (6) yields:

$$w_i = w_j = w = (p_i + p_j)/2\cos(\beta) \qquad\qquad (7)$$

When the magnitude and angle from horizontal of the total velocity vectors are known, the beam parallel components are given by:

$$p_i = u_i \sin(\beta + \mathrm{atan}(w_i/h_i)) \qquad\qquad (8a)$$

$$p_j = -u_i \sin(\beta - \mathrm{atan}(w_j/h_j)) \qquad\qquad (8b)$$

where $\mathrm{atan}(w_i/h_i)$ and $\mathrm{atan}(w_j/h_j)$ are equivalent to the angles from horizontal of the total velocity vectors in beams i and j.

Some aspects of how variability in the flow field affects velocity measurements and the detection of velocity errors in a 4-beam ADCP can be deduced from equations (4) through (8). Because each beam pair in a 4-beam system independently generates an estimate for the vertical velocity component, the assumption of homogeneous flow can be tested by comparing the two vertical velocity estimates. Any difference between w from one beam pair and w from the other beam pair indicates that errors may exist in the horizontal velocity estimates. This difference in vertical velocity components is termed the "error-velocity." Instrument firmware is designed so reject bin measurements for which the error-velocity exceeds a use-specified threshold.

However, some types of flow heterogeneities produce errors that cannot be detected using the error-velocity criteria. This can occur when the flow is such that the vertical velocity components in both beam pairs are unaffected by the flow heterogeneities, or contain similar errors in both beam pairs. For example, consider a heterogeneous velocity field with all velocity components still in the plane containing beam i and beam j, but with the total velocity vectors describing a concave-up arc as shown in Fig. 15. Total vector magnitudes are equal at 0.5 m/s, but the flow vector in beam i is directed downward at an angle of $-8°$ from horizontal, and the vector in beam j is directed upward at an angle of $8°$. Both horizontal velocity components are thus equal to 0.495 m/s, the vertical components w_i and w_j are -0.07 m/s and 0.07 m/s, respectively, and the beam-parallel components p_i and p_j are 0.104 m/s and -0.104 m/s. According to equation (4), these values of p_i and p_j imply a horizontal velocity of 0.304, which is in error relative to the actual horizontal velocity in the two beams by 0.191 m/s, or about 36%. However, because p_i and p_j are equal in magnitude and opposite in sign, the numerator of equation (7) and the measured vertical velocity is zero. The flow vectors intersecting the other beam pair (shown by the dashed line in Fig. 15) are orthogonal to the plane containing that beam pair, and have no vertical or beam-parallel velocity component. Thus,

17

the other pair also registers zero horizontal and vertical velocity, and the reported error-velocity will be zero, despite the presence of a significant horizontal velocity error.
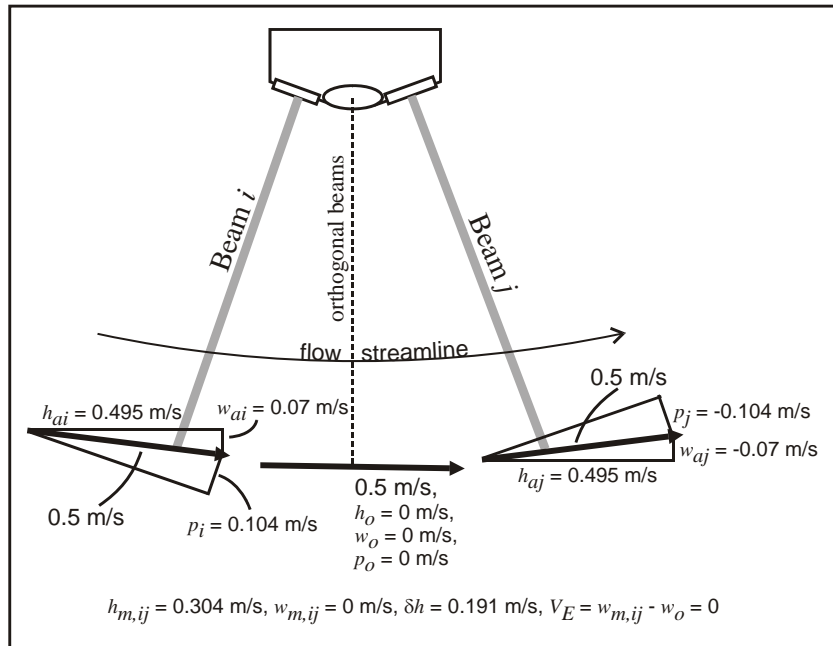

Figure 15. Diagram showing the effect of a concave-up flow velocity field on measured flow velocity and the error velocity. Subscripts are as follows: ai, and aj indicate the actual velocity components in beams i and j; m,ij indicates the measured velocity components in beams i and j obtained from equations (4) and (7); o indicates the horizontal velocity in the orthogonal plane and all velocity components measured by the orthogonal beams. δh is the actual horizontal error in the plane containing beams i and j, V_E is the error velocity, and all other symbols are as previously defined.

Moving-bed Conditions

Vertical heterogeneities in the flow field may be especially problematic when making bottom-track measurements in the presence of a moving bed. Bedload transport is known to be highly spatially variable over distances similar to or smaller than the lengths of individual bedforms (Gomez and Troutman 1997, Fig. 3). Given the close proximity of areas with different bedload transport rates on a stream bed, it is likely that different bottom velocities are frequently observed in different beams from the same ADCP. Flow heterogeneities can be with respect to the horizontal flow velocity, the vertical flow velocity, the concentration of the moving material reflecting the beams, or all three. Streamlines of bedload motion at the bed are presumably oriented parallel to the bed surface, and therefore rise and fall according to the bed topography. Bed slopes associated with dunes have been reported in the range of about 2-7° for stoss faces (Kostaschuk and Villard 1996), and are typically about 30° for lee faces (Gomez and Troutman 1997). Although it is difficult to separate real temporal variability in moving-bed velocities from noise caused by spatial variability, we suggest that the latter accounts for a large portion of the considerable variability observed in acoustic moving-bed measurements.

Conclusions

When mounted on a boat or other moving platform, ADCPs can be used to map a wide range of ecologically significant phenomena. In addition to specifying environmental conditions at discrete locations, spatially-explicit 3-dimensional flow velocity information is useful for defining environmental gradients and investigating multi-scale ecosystem organization. Velocity data can be processed or combined with other environmental variables to produce measures of fluid shear, turbulence, or vorticity. Comparisons between bottom-track velocity measurements and instrument velocities determined by GPS can be used to estimate flow velocities within a few cm of the bed, and to identify areas where the benthic environment is unstable and persistently battered by sediment particle impacts.

Many of the potential errors affecting ADCP data are the direct result of instrument motion. The greater the mobility of the instrument platform, the greater is the potential for large moving-platform errors. Moving-platform error sources with significant potential to affect ADCP velocity measurements include velocity ambiguity errors and compass errors. Because bed velocities can be much lower than typical water column velocities, their measurement is especially sensitive to all types of moving-platform errors.

Compass calibration errors refer to a persistent mis-alignment between magnetic north as measured by the instrument's internal compass and geographic north. Although these errors can be minimized by proper compass calibration using procedures specified by the equipment manufacturer (see, for example, RD Instruments, Inc. 2002), it is nonetheless also necessary to pay careful attention to absolute instrument velocity during mapping operations. Analyses presented in this report demonstrate that relatively minor mis-alignment of the compass can produce significant velocity errors, depending on the ratio of absolute instrument velocity to the target velocity and on the relative directions of instrument and target motion. Limiting absolute instrument velocities to about 1 m/s should ensure that minor compass mis-alignments will not generate errors of more than about 0.02 m/s under most operating conditions. In addition to amplifying the effects of compass errors, high boat velocities can result in large dynamic compass errors caused by instrument accelerations. Velocity anomalies recorded during high-speed boat maneuvers indicate that motions such as turning the boat can produce erroneous velocity measurements.

The potential for generating velocity ambiguity errors is related to the velocity of the instrument relative to the water flow rather than the absolute instrument velocity. It is recommended that relative water speeds should not be allowed to exceed the horizontal ambiguity velocity for which the instrument is configured, minus a safety factor to accommodate instrument noise. We suggest two times the single ping standard deviation for instrument noise, as determined for the instrument configuration in use, as an appropriate safety factor. To minimize relative water velocities, data collection while moving upstream against strong currents should be avoided.

Velocity errors produced by spatial variability in the flow field are typically controlled using an error-velocity threshold. However, some flow-field configurations can generate velocity errors without also producing a high error-velocity. Errors caused by heterogeneous flow may be particularly problematic when measuring the velocity of sediment moving near the stream bed.

Acknowledgements

19

Literature Cited

Deines, K.L., undated, *Backscatter estimation using broadband acoustic Doppler current profilers*, RD Instruments, Inc., Application Note FSA-008.

Gomez, B. and B.M. Troutman, 1997, Evaluation of process errors in bed load sampling using a dune model, *Water Resources Research* 33(10):2387-2398.

Jacobson, R.B., M.S. Laustrup and J.M Reuter, 2002, *Habitat Assessment, Missouri River at Hermann, Missouri*. U.S. Geological Survey Open File Report 02-32, 22 pp.

Jowett, I.G., 1993, A method for objectively identifying pool, run, and riffle habitats from physical measurements, *New Zealand Journal of Marine and Freshwater Research* 27:241-248.

Joyce, T.M., 1989, On *in situ* 'calibration' of shipboard ADCPs, *Journal of Atmospheric and Oceanic Technology* 6:169-172.

Kostaschuk, R. and P. Villard, 1996, Flow and sediment transport over large subaqueous dunes: Fraser River, Canada, *Sedimentology* 43:849-863.

Mueller, D.S., 2003, Field evaluation of boat-mounted acoustic Doppler instruments used to measure streamflow, *Proceedings of the IEEE 7th Working Conference on Current Measurement*, Institute of Electrical and Electronics Engineers, Piscataway, NJ.

Poff, N.L. and J.V. Ward, 1990, Physical habitat template of lotic systems: recovery in the context of historical pattern of spatio-temporal heterogeneity, *Environmental Management* 14:629-645.

RD Instruments, Inc., 1996, *Principles of operation: A practical primer, 2nd Edition for Broadband ADCPs*. RD Instruments, Inc., San Diego, CA.

RD Instruments, Inc., 2002, *Workhorse Rio Grande ADCP User's Guide,* RD Instruments, Inc., San Diego, CA.

Rennie, C.D. and R.G. Millar, 2004, Measurement of the spatial distribution of fluvial bedload transport velocity in both sand and gravel, *Earth Surface Processes and Landforms* 29:1173-1193, doi:10.1002/esp.1074.

Rennie, C.D., R.G. Millar and M.A. Church, 2002, Measurement of bed load velocity using an acoustic Doppler current profiler, *Journal of Hydraulic Engineering* 128(5)473-483.

Rehmel, M.S., J.A. Stewart and S.E. Morlock, 2003, Tethered acoustic Doppler current profiler platforms for measuring streamflow, U.S. Geological Survey Open File Report 03-237. 15 pp.

Shields, F.D., Jr., S.S. Knight, S. Testa, III, and C.M. Cooper, 2003, Use of acoustic Doppler current profilers to describe velocity distributions at the reach scale, *Journal of the American Water Resources Association* 39(6):1397-1408.

Simpson, M.R., 2001, *Discharge measurements using a broad-band acoustic Doppler current profiler,* U.S. Geological Survey Open File Report 01-1. 123 pp.

Townsend, C.R., 1989, The patch dynamics concept of stream community ecology, *Journal of the North American Benthological Society* 8:36-50.

US Geological Survey, 2001, *Office of Surface Water Technical Memorandum no. 2002.02,* Office of Surface Water, Water Resouces Division.

Ward, J.V., K. Tockner and F. Schiemer, 1999, Biodiversity of floodplain river ecosystems: ecotones and connectivity, *Regulated Rivers: Research and Management* 15:125-139.